Deep levels of copper-hydrogen complexes in silicon

Nikolai Yarykin*
Institute of Microelectronics Technology, Russian Academy of Sciences, 142432 Chernogolovka, Russia

Jörg Weber
Technische Universität Dresden, 01062 Dresden, Germany
(Received 19 April 2013; published 14 August 2013)

Complexes of substitutional copper (Cu_s) with hydrogen in silicon are investigated by standard deep-level transient spectroscopy (DLTS) and high-resolution Laplace-transform DLTS. Hydrogen is introduced into the near-surface layer of copper-doped crystals during wet chemical etching and moved deeper into the sample by annealing Schottky contacts under reverse bias at 350–380 K. Two novel centers are observed to form in the hydrogenated region. Each of them possesses two deep levels which are only slightly different from the Cu_s levels. Analysis of the depth profiles allows us to identify the observed centers as complexes of Cu_s with one and two hydrogen atoms and reveals the formation of an electrically inactive complex with three hydrogen atoms. The identification is confirmed by the numerical modeling of the copper-hydrogen interaction which enables a quantitative description of the experimentally measured concentrations of different complexes. The variations of the Cu_s donor and acceptor levels due to successive hydrogenation are found to be similar to those for isoelectronic Ag and Au impurities.

DOI: 10.1103/PhysRevB.88.085205 PACS number(s): 71.55.Cn, 61.72.J−, 61.72.Yx

I. INTRODUCTION

In silicon, the electronic structures of the substitutional transition metals (TM's) near the end of the 3*d*, 4*d*, and 5*d* series are interpreted on the base of the so-called vacancy model.[1] The model assumes a filled *d* shell deep in the valence band with the remaining electrons in the vacancylike orbitals of the four silicon neighbors, which are in the forbidden gap and account for the electrical activity of the defect. In the model, only a small admixture of the *d* electrons should be present in the vacancylike orbitals. Most of the available electron paramagnetic resonance results were successfully explained by the vacancy model.[2]

In contrast, recent *ab initio* calculations predict that substitutional copper (Cu_s) does not retain its closed *d* shell but promotes some *d* electrons to the 4*sp* shell and forms covalent bonds with four Si neighbors.[3] These calculations adequately reproduce the experimentally measured deep-level (DL) pattern of the Cu_s defect.[4,5]

More information on the electronic structure of TM's could come from the addition of extra electrons to the system by formation of the TM complexes with hydrogen. It was experimentally observed that three or four hydrogen atoms are required for a full passivation of the TM's with filled or almost-filled *d* shells (Au, Pt, Ag, and Pd), while a smaller number of hydrogen atoms results in new deep levels.[6–10] This behavior seems to be a general property of isolated substitutional TM's and was first studied in Ge on the Cu_s triple acceptor.[11]

The DL patterns of the TM-hydrogen complexes in Si reveal similarities inherited from isolated isoelectronic TM's.[9,12] Moreover, the DL variations due to the increment of the number of hydrogen atoms are found to be distinctive for the given group in the Periodic Table. Nearly identical DL positions were found for the Pd-H and Pt-H complexes with an equal number of hydrogen atoms (Ref. 10, Figs. 11 and 12), while diverse (but similar to each other) DL variations were observed for hydrogenated Au and Ag (Ref. 9, Fig. 11).

Therefore, the behavior of the Cu_s DL pattern under hydrogenation is expected to be similar to those for Ag and Au. However, the centers identified as the Cu-H_1 and Cu-H_2 complexes exhibit quite different level positions (Ref. 13, Fig. 7). The reason for this dissimilarity was unclear until recently, when some of the levels ascribed in Ref. 13 to Cu-H complexes were shown not to contain hydrogen.[14]

In the present study we investigate formation of the Cu-H complexes with a special attention to the correlation between the DL depth profiles and the hydrogen concentration. Use of reverse-bias annealing (RBA)[15] in *p*-type samples allows us to form well-defined hydrogen distributions and to make a quantitative comparison with the results of numerical modeling.

II. EXPERIMENTAL DETAILS

A. Samples

The experiments were performed on *p*-type Si single crystals grown by the float-zone technique (boron concentration $\sim 10^{15}$ cm^{-3}). Copper was introduced during the crystal growth as described in Ref. 13. The DL spectrum of the as-received wafers was dominated by the $E_v + 0.1$ eV level, which was ascribed to the Cu-related complex which gives rise to the photoluminescence line at 1014 meV.[16] (This defect was recently observed to contain four copper atoms.[17]) Annealing at 350 °C for 30 min terminated by fast cooling reduced the concentration of the copper complex below $\sim 5 \times 10^{11}$ cm^{-3} and generated the substitutional copper levels with a concentration of $\sim 7 \times 10^{13}$ cm^{-3}. There were no signs of mobile Cu_i species present in the volume of the annealed samples.

After annealing, all samples were chemically etched in the mixture of acids ($HF : HNO_3 : CH_3COOH = 1 : 2 : 1$). The treatment in this solution for 1 min at room temperature removed a layer about 20 μm from each side. Schottky diodes with a diameter of 1.6 mm were formed on the etched surface by thermal evaporation of aluminum. The Ohmic contacts

 ©2013 American Physical Society

were made by scratching the back surface with an eutectic In-Ga alloy.

B. Capacitance techniques

An *LCR* meter operated at 1 MHz was used for capacitance-voltage (CV) measurements. Standard DLTS measurements were performed in the temperature range 40–340 K with a modified Boonton 72B capacitance meter and a lock-in amplifier with sine correlation function. Typically, the filling pulse duration and the setup rate window were set to 1 ms and 49 s^{-1}, respectively. The DLTS curves presented below are the lock-in output normalized by a factor $V_r/(V_r - V_p)$, where V_r and V_p are the reverse bias and filling pulse voltages, respectively. By this method, the levels with equal concentrations provide DLTS peaks of approximately the same amplitude.

Using the standard DLTS setup, the DL depth profiles were calculated from the signal dependence on the filling pulse amplitude at a fixed reverse bias. The inhomogeneous net boron profiles, which were determined from the CV measurements, and the so-called λ layer[18] were properly included in the calculations. The quasistationary (under reverse bias) and dynamic (during the filling pulse) widths of the λ layers were calculated using the activation energies and apparent capture cross sections obtained from the Arrhenius plots for the hole emission rates.

We applied Laplace-transform DLTS (LDLTS)[19] to resolve overlapping DLTS peaks, to precisely determine their activation energies and to measure the depth profiles of the levels with similar emission properties. In the last case, the double-DLTS[20] approach was employed, i.e., the signal from a narrow depth region was calculated as a difference of two capacitance transients measured with close pulse voltages and the same reverse bias. The DL depth profiles were calculated by integrating the areas under each LDLTS peak with the geometrical factors used for standard DLTS profiling. The LDLTS setup operated in the temperature range 80–300 K.

III. RESULTS

A. Wet chemically etched samples

The DLTS spectra of the sample which was subjected to wet chemical etching (WCE) at room temperature are shown in Fig. 1(a). The solid and dashed curves were taken under bias conditions which correspond to the depth regions 0.8–1.7 and 2.8–3.6 μm, respectively. The net boron depth profile calculated for this sample from the CV measurements is shown in Fig. 2 (curve WCE in the upper part). Its reduction closer to the surface results from the hydrogen passivation and indicates the depth of hydrogen penetration during etching. Therefore, the two depth regions probed by DLTS in Fig. 1(a) correspond to the hydrogenated and hydrogen-free regions, respectively.

The DL spectrum in the hydrogen-free region is dominated by three peaks denoted as Cu_{100}, Cu_{220}, and Cu_{270}. (In the Cu_{xxx} notation the subscript indicates the approximate temperature at which the peak maximum occurs under standard measurement conditions, i.e., a rate window of 49 s^{-1} in our case.) The Cu_{100} and Cu_{220} peaks are usually related to DLTS signatures of the donor and acceptor levels of the isolated substitutional copper atom (Cu_s), respectively. The Arrhenius curves for the hole emission rates from these levels were measured by LDLTS and are in a close correlation with the earlier results.[21–23] Use of the LDLTS technique is especially important for the Cu_s donor level to separate it from the Cu_{102} level with similar emission properties.[14]

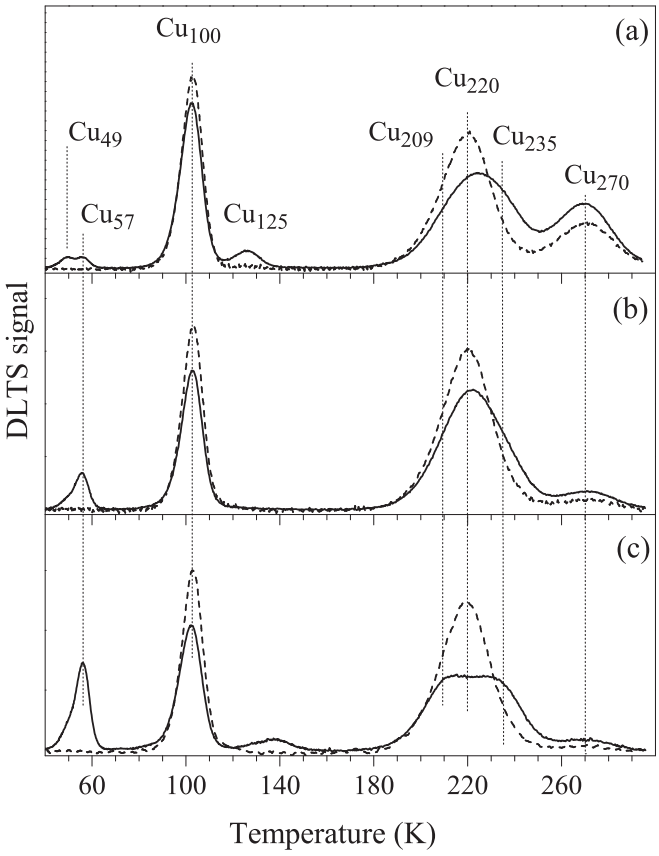

FIG. 1. DLTS spectra of a Cu-doped sample after wet chemical etching (a) and subsequent reverse-bias annealings at 360 K for 40 min (b) and an additional 80 min (c). The spectra are taken either from the hydrogen-free region [deeper than ~3 μm for frame (a) and 4 μm for frames (b), (c)] (dashed curves) or from the hydrogenated layer at 1–3 μm in depth (solid curves) (see the net boron depth profiles in Fig. 2). The rate window is 49 s^{-1}.

A defect with the Cu_{102} and Cu_{270} levels was earlier related to the Cu-H_1 complex[13] but has recently been ascribed to the Cu_s-Cu_i pair.[14] As created by chemical etching, the defect is localized at the surface but penetrates much deeper than hydrogen. The curves in Fig. 1(a) as well as the depth profiles of the DLTS peaks (not shown here) closely resemble those measured in similar samples after wet chemical etching (Ref. 13).

Closer to the etched surface [solid curve in Fig. 1(a)] a relatively strong Cu_{235} signal overlapped with Cu_{220} and weaker Cu_{49}, Cu_{57}, and Cu_{125} peaks are detected. The Cu_{125} level was related to the Cu-H_2 complex.[13] However, the Cu_{49} and Cu_{125} centers, similar to Cu_{270}, can also be detected in the hydrogen-free region. Therefore, only the Cu_{57} and Cu_{235} levels could belong to the hydrogen-related complexes.

B. Reverse-bias annealing

It is known from earlier investigations of hydrogen interaction with different TM's in *p*-type silicon [6,8–10] that

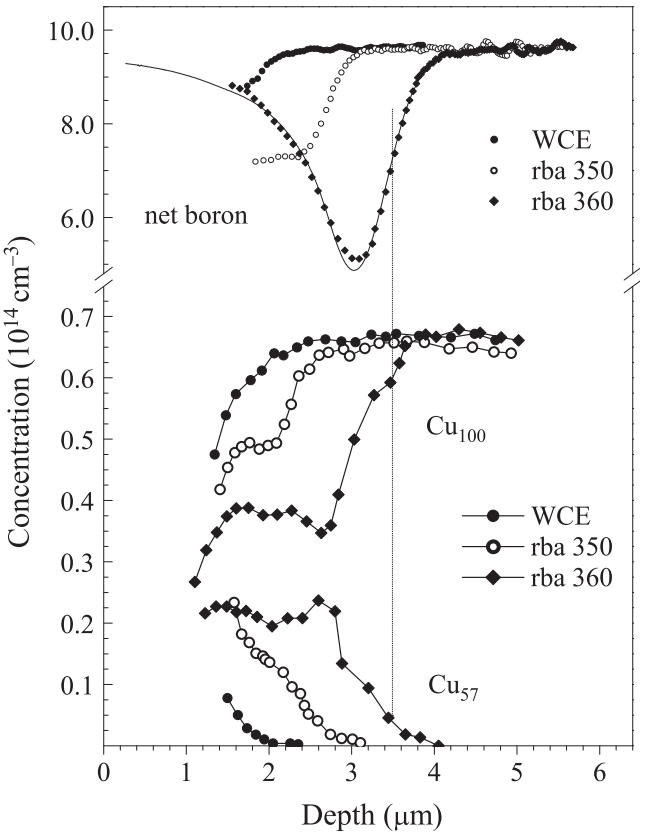

FIG. 2. Experimental concentration depth profiles for the net active boron (top) and the Cu_{100} and Cu_{57} peaks (bottom) after the wet chemical etching at room temperature and subsequent reverse-bias annealings at 350 K for 100 min and then at 360 K for 120 min. The solid line in the upper part is a result of numerical simulation (Sec. IV B). Note the scale variation at the y-axis break.

chemical etching at room temperature forms a limited amount of hydrogen-related complexes located very close to the surface, in the region which is hardly accessible by DLTS. The same is found in our samples; for example, a measurable concentration of the Cu_{57} centers is observed only at the depth at which no reliable CV data are available (Fig. 2). Therefore, the procedure of reverse-bias annealing (RBA)[15] was applied to move hydrogen deeper into the crystal and stimulate its interaction with copper.

The DLTS spectra taken after two successive RBA steps are shown in Figs. 1(b) and 1(c). Growth of the Cu_{57} level and some decrease of the Cu_{100} peak in the hydrogenated region are the most prominent effects after the early stages [Fig. 1(b)]. The Cu_{57} center is not formed and the Cu_{100} amplitude remains stable deeper in the crystal, where the hydrogen concentration is low. Another significant impact of the RBA treatments is a drastic reduction of the Cu_{270} peak. However, the Cu_{270} annealing proceeds similarly at different depths and seems to be independent of the hydrogen concentration. Also, the Cu_{125} feature totally disappears after a short annealing at 350 K.

Longer RBA treatments result in a further growth of the Cu_{57} level and changes of the DLTS signal around 220 K. The solid curve in Fig. 1(c) clearly shows the presence of a novel level denoted as Cu_{209}. The broad feature at ~140 K was only observed rather close to the etched surface after the longest RBA treatments. Its nature is unknown.

The evolution of the Cu_{57} and Cu_{100} depth distributions measured by the standard DLTS profiling is shown in Fig. 2. These profiles demonstrate an obvious anticorrelation, implying that the Cu_{57} center is formed at the expense of Cu_s. At later stages of hydrogenation, the sum $[Cu_{57}] + [Cu_{100}]$ (brackets indicate the concentration values) exhibits some deficit (to 20–25% of the initial Cu_{100} concentration) in the region where the Cu_{57} level is formed. This suggests that further defect formation takes place.

The Cu_{57} and Cu_{100} depth profiles correlate with the net boron distributions obtained from the CV data (Fig. 2). For all RBA stages, the position where the B-H pair concentration reaches half of its maximum value corresponds to the depth at which the Cu_{57} level concentration drops to zero. (The position for the last anneal is shown by the vertical dotted line in Fig. 2.) We revert to the nature of this shift in Sec. IV B.

C. Laplace-DLTS results

The resolution of our standard DLTS is insufficient to fully separate the overlapping peaks around 220 K and to measure the depth distributions of the corresponding centers with acceptable accuracy (see Fig. 1). Therefore, the high-resolution Laplace-DLTS technique (LDLTS) [19] was applied to the hydrogenated samples.

The capacitance transients taken from the hydrogenated region in the temperature range 190–250 K are easily resolved into three LDLTS peaks denoted as Cu_{209}, Cu_{220}, and Cu_{235} (Fig. 3). (In accordance with the previous use, subscripts in the Cu_{xxx} notation for LDLTS peaks indicate at which temperature the hole emission rate is equal to 49 s^{-1}.) The activation energies and apparent capture cross sections of the

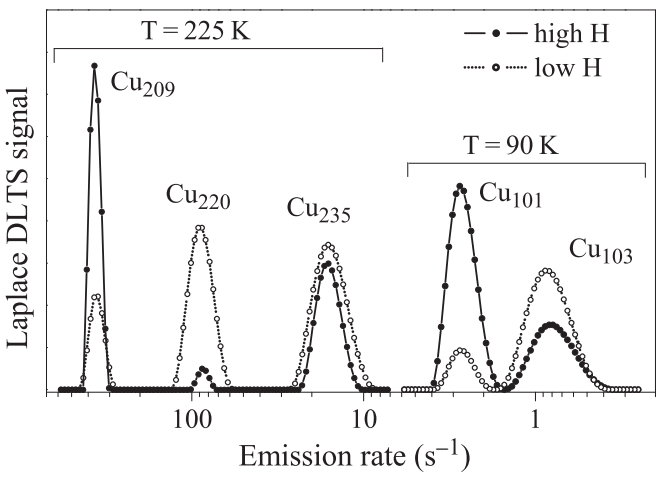

FIG. 3. LDLTS spectra measured at 225 and 90 K in the sample which was chemically etched at room temperature and annealed at 380 K for 20 min without bias and then at 370 K for 100 min under a reverse bias of 6 V. The curves with solid symbols were measured from the regions with high hydrogen concentration (around 0.9 μm at 225 K and 1.2 μm at 90 K, respectively). The curves with open symbols were taken from the hydrogen-lean region (around 3.2 μm for both temperatures). Note the inverted abscissa axis.

TABLE I. Activation energies E_A, apparent hole capture cross sections σ_p, and assignments of the observed levels.

Notation	E_A (meV)[a]	σ_p (cm^{-2})[b]	Assignment
Cu_{103}	225 ± 4	1.4×10^{-13}	$Cu_s^{(0/+)}$
Cu_{220}	430 ± 4	2.0×10^{-15}	$Cu_s^{(-/0)}$
Cu_{57}[c]	104 ± 7	8×10^{-15}	Cu_s–$H_1^{(0/+)}$
Cu_{235}	491 ± 8	1.0×10^{-14}	Cu_s–$H_1^{(-/0)}$
Cu_{101}	194 ± 4	7.4×10^{-15}	Cu_s–$H_2^{(0/+)}$
Cu_{209}	462 ± 7	4.5×10^{-14}	Cu_s–$H_2^{(-/0)}$

[a]The shown uncertainty includes both the point scattering on the Arrhenius plots and the sample-to-sample variations.
[b]Calculated from the Arrhenius plot for emission rates with $\upsilon_{th} N_v = 3.3 \times 10^{21}$ T^2 cm^{-2} s^{-1}.
[c]From the standard DLTS data.

corresponding levels were obtained from the emission rates measured at different temperatures (see Table I).

Taking the LDLTS spectra at different depth regions (two spectra are shown in Fig. 3) the DL depth profiles were calculated as described in Sec. II B (Fig. 4). The concentration of the Cu_s acceptor level (Cu_{220}) is rather low around 1 μm in depth, in apparent contradiction with the much higher concentration calculated from the Cu_{100} DLTS signal at the same depth (see Fig. 2). A similar inconsistency between the Cu_{100} and Cu_{220} peak amplitudes is seen for the solid line in Fig. 1(c).[24] These observations suggest that the Cu_s donor level is not the only contributor to the Cu_{100} DLTS peak. Indeed, careful LDLTS measurements showed that the capacitance transients taken at 87–110 K can be resolved into two components, Cu_{101} and Cu_{103} (Fig. 3 and Table I).

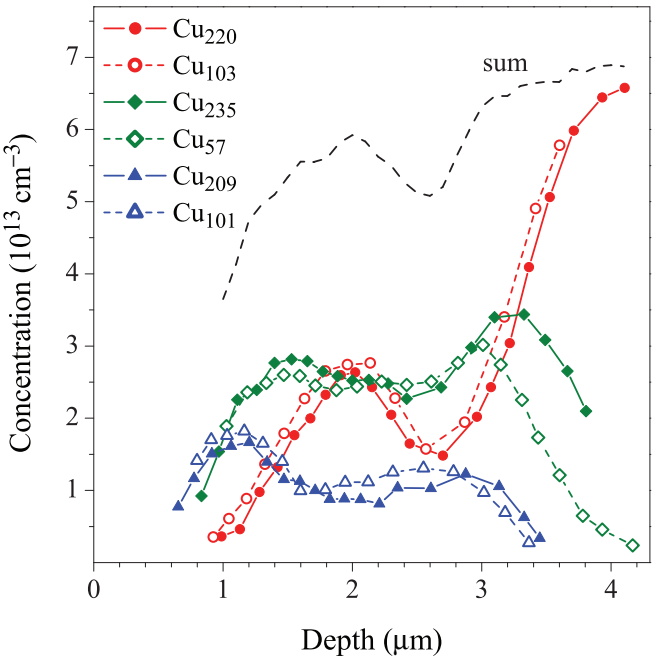

FIG. 4. (Color online) Concentration depth profiles of the main Cu-related deep levels measured by the LDLTS technique (Cu_{57} from the standard DLTS data). The dashed line shows the sum of Cu_{220}, Cu_{57}, and Cu_{209} concentrations. For the sample treatment, see the caption for Fig. 3.

The Cu_{103} signal dominates in the region with low hydrogen concentration and, therefore, is assigned to the Cu_s donor level. The Cu_{101} component is observed only in the hydrogenated layers and is related to the copper-hydrogen complex. The depth profiles of these levels are also shown in Fig. 4.

IV. DISCUSSION

A. Pairwise correlation of the DL depth profiles

The six depth profiles shown in Fig. 4 are naturally grouped in three pairs, implying the presence of three different centers. Each center possesses two levels: a shallower one (with temperatures of the DLTS peak maxima $T_m \leqslant 103$ K) and a deeper one ($T_m \geqslant 209$ K). Cu_{103} and Cu_{220} correspond to the donor and acceptor levels of Cu_s, respectively. The second pair consists of the Cu_{57} and Cu_{235} levels, and the third pair comprises the Cu_{101} and Cu_{209} levels. A similar behavior was observed in all samples in which the DL depth profiles were analyzed with LDLTS after the RBA treatments. We identify the Cu_{57}/Cu_{235} and Cu_{101}/Cu_{209} centers as copper-hydrogen complexes.

The most obvious discrepancy between the concept of pairwise correlation and the experimental DL profiles in Fig. 4 is the difference in the Cu_{57} and Cu_{235} concentrations at 3–3.8-μm depth. Whereas the profiles coincide inside the space-charge region (SCR) which existed during the defect formation, Cu_{235} increases around the SCR boundary in all studied samples. A much stronger Cu_{235} signal (as compared to Cu_{57}) could also be seen immediately after chemical etching without any RBA treatment [Fig. 1(a)]. We believe that the higher concentration of the Cu_{235} levels is determined by the presence of another center, although the LDLTS investigations were unable to separate the hole emission from this additional level. Note, however, that the Cu_{235} peak in the spectrum taken at 225 K for the layer around 3.3 μm (marked as *low H* in Fig. 3) is apparently wider than that for the 1–1.2-μm layer (*high H*).

According to the above discussion, the sum concentration S of the Cu_{220}, Cu_{57}, and Cu_{209} levels was used as an indicator of the Cu_s balance (dashed line in Fig. 4). The S depth profile is nearly flat between 3 and 4 μm in spite of strong variations of the constituents. For example, the concentration of isolated Cu_s atoms drops down to ~30% of its initial value at the depth around 3 μm, while S is reduced by ~5% only. This indicates that the Cu_{57}/Cu_{235} and Cu_{101}/Cu_{209} centers are formed at the expense of Cu_s. We relate these centers to the Cu_s complexes with one and two hydrogen atoms, respectively.

This identification of the number of hydrogen atoms involved in the defects comes from the analysis of depth profiles at the end of the hydrogenated region where hydrogen concentration is low. Under such conditions the concentration of the complex with one hydrogen atom has always to dominate over all other complexes (e.g., see Fig. 9 in Ref. 9). In all our experiments the Cu_{57} levels could be detected in deeper layers than the Cu_{101}/Cu_{209} centers (3.5–4-μm interval in Fig. 4).

The sum concentration of all three centers shows an evident decrease in the regions of the strongest hydrogenation around 2.5 and 1 μm (Fig. 4). This strongly suggests that up to 25% of the Cu_s atoms in these layers are involved in the complexes

which include three (or more) hydrogen atoms and have no deep levels in the lower half of the gap.

Note also that the S value would essentially exceed the initial Cu_s concentration if the sum concentration were calculated using the Cu_{235} level concentration instead of Cu_{57}. The additional underlying center of the Cu_{235} signal, which is found between 3 and 4 μm in Fig. 4, can therefore not be related with a Cu_s defect.

B. Quantitative description of the DL profiles

Assuming that copper-hydrogen complexes are thermally stable at the considered temperatures, their formation can be described by the following set of equations:[9]

$$\frac{dN_0}{d\Phi} = -r_0 N_0, \tag{1}$$

$$\frac{dN_i}{d\Phi} = r_{i-1}N_{i-1} - r_i N_i, \quad i = 1,2,3\ldots, \tag{2}$$

where N_0 is the Cu_s concentration, N_i is the concentration of the Cu_s-H_i complexes, r_i is the radii of hydrogen capture to the corresponding defects, and Φ is the *integral hydrogenation* (introduced in Ref. 9 as a local hydrogenation time). The solution of Eqs. (1) and (2) is straightforward and the problem is reduced to the estimation of Φ at each given depth.

The integral hydrogenation Φ is determined as[9]

$$\Phi = \int_0^t 4\pi D_{\mathrm{H}}[\mathrm{H}]dt = \int_0^t \frac{\nu_{\mathrm{BH}}}{r_{\mathrm{BH}}}\frac{B_0 - [\mathrm{B}]}{[\mathrm{B}]}dt. \tag{3}$$

Here, D_{H} and [H] are the diffusivity and concentration of free (noncaptured) hydrogen, r_{BH} is the radius of hydrogen capture to boron, ν_{BH} is the B-H dissociation rate, and B_0 and [B] are the initial (uniform) boron doping and the concentration of active (nonpassivated) boron, respectively. The expression at right in Eq. (3) is valid for local equilibrium between the formation and dissociation of the B-H pairs at the RBA temperature.[9] The latter formula clearly shows that Φ is practically independent of D_{H}, which is known with a great uncertainty. Since the parameters of boron-hydrogen interaction (r_{BH} and ν_{BH}) are known,[15] Φ can be, in principle, estimated from the experimental CV profiles. However, this approach requires numerous (but short) RBA steps for accurate Φ estimation.

In this work, the integral hydrogenation Φ was calculated by numerical modeling of the hydrogen penetration during RBA. Similar to Ref. 15, the modeling describes the drift and diffusion of positively charged hydrogen taking into account the boron-hydrogen interaction and a spatially inhomogeneous distribution of holes and ions. (The copper-hydrogen interaction can be omitted during the modeling of hydrogen penetration since the Cu_s concentration is low compared to that of boron.) Since all the experimental parameters (applied bias and RBA temperature and duration) are known, there is only one critical fitting value: the total amount of hydrogen injected into the sample during WCE. (The details of hydrogen distribution inside the near-surface layer after WCE have only a small impact on the final B-H profile.) The proper adjustment of this value results in the calculated profile of the net boron concentration shown in Fig. 2 with a solid line. The modeling

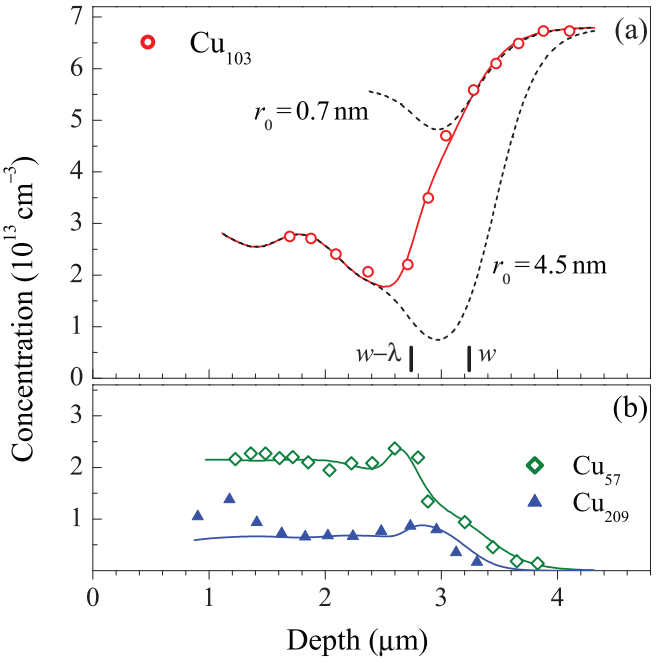

FIG. 5. (Color online) The experimental depth profiles (symbols) measured after the final RBA step (the experimental conditions are given in the caption for Fig. 2) for the Cu_{103} (a) and Cu_{57} and Cu_{209} (b) levels. The dashed curves are given by Eq. (4) for the constant r_0 values indicated on the plot. The solid curves were calculated using the effective capture radii (see text) with the parameters listed in Table II. The short vertical lines in the (a) frame indicate the position of the λ layer for the Cu_s acceptor level just before the termination of the RBA treatment.

closely reproduces the experimental profile and confirms that boron passivation in our experiments is caused by hydrogen.

Equation (1) assumes that the disappearance of the Cu_s levels is governed by the single parameter r_0, the radius of the copper–hydrogen interaction:

$$N_0 = N_0^{\mathrm{ini}} \exp(-r_0\Phi), \tag{4}$$

where N_0^{ini} is the initial Cu_s concentration. (Φ was calculated for each depth during the modeling of hydrogen penetration.) The fitting of the experimental Cu_s depth profile after the RBA treatment by Eq. (4) is illustrated in Fig. 5(a) with dashed lines. It is seen that quite different r_0 values are required to fit the experimental points in the 1.7–2.2- and 3.1–3.7-μm depth regions. Note, however, that the obtained values (4.5 and 0.7 nm, respectively) are typical of the H^+ capture by negatively charged and neutral impurities, respectively.[9,15,25] Indeed, the Cu_s acceptor level is located in the lower half of the band gap at $E_v + 0.43$ eV. This is above the Fermi-level position in the quasineutral volume at the RBA temperatures ($\sim$0.3 eV at 350–380 K). Therefore, Cu_s is mainly neutral deeper than the $(w - \lambda)$ depth (w is the position of the SCR boundary, and λ is the width of the transition layer[18]) and negatively charged closer to the surface.

We introduce the position-dependent effective capture radius, calculated as

$$r_0^{\mathrm{eff}}(\mathrm{x}) = [1 - f(\mathrm{x})]\, r_0^0 + f(\mathrm{x})\, r_0^-, \tag{5}$$

TABLE II. Radii of hydrogen capture to the Cu-related centers in neutral (r^0) and negative (r^-) charge states.

Centers	r^0 (nm)	r^- (nm)
Cu_s	0.5	4.5
Cu_s-H_1	3	6
Cu_s-H_2	2	18

where r_0^0 and r_0^- are the capture radii for neutral and negative Cu_s, respectively, and $f(x)$ is the filling factor of the Cu_s acceptor level. The latter is given by the Fermi function and the band bending calculated during the modeling and does not introduce any additional fitting parameters.

Substitution of $r_0^{\text{eff}}(x)$ for r_0 in Eq. (4) with properly adjusted r_0^0 and r_0^- values (see Table II) produces the curve which deviates from the experimental Cu_s depth profile by 8% at most in the whole depth interval [solid curve in Fig. 5(a)]. Note that both dashed lines in Fig. 5(a) exhibit the minima at ~3 μm, where Φ has a maximum. However, the minimum Cu_s concentration (Cu_{103} level) is observed closer to the surface. The main reasons for this shift (emphasized also by the vertical line in Fig. 2) are the large r_0^-/r_0^0 ratio and the existence of the λ layer, which was about 0.5 μm during the RBA treatments.

Both copper-hydrogen complexes possess deep levels which are close to the Cu_s acceptor and, consequently, have to change their charge state inside the analyzed region. Therefore, their depth profiles were also fitted using the effective capture radii [see Table II and Fig. 5(b)]. It is seen that the concept of the position-dependent capture radius allows a very close description of the experimental DL depth profiles. The only significant deviation is a few points in the Cu_{209} profile at the 0.9–1.4-μm depths. The reason for this is not clear at the moment. In all cases the r^- capture radii are larger than the corresponding r^0 values. This is in agreement with the fact that the complexes are more negative (more attractive for H^+) inside the SCR as compared to the quasineutral p-type volume.

Fitting of the Cu-H_2 depth profile requires nonzero r_2 capture radii (third line in Table II), indicating the Cu-H_3 formation. This confirms the conclusion drawn in the previous section from the analysis of the sum concentration of the electrically active copper-hydrogen centers.

C. Comparison with the theory and other TM's

The properties of copper-hydrogen complexes were calculated by two different groups.[3,4] In spite of different methods used (molecular dynamics and density functional, respectively), both studies predict the same structure of the complexes: Hydrogen atoms were found to bind directly to Cu_s, inducing minimal stresses to the lattice. As a result, the binding energies for the first, second, and third hydrogen atoms in the complex are nearly equal to each other (~2.3 eV in Ref. 3 or ~1.7 eV in Ref. 4). These rather high values imply a thermal stability of the Cu_s-H_n complexes to 250–450 °C. The formation of a complex with four hydrogen atoms is not expected.

Modeling of our RBA treatments at 350–380 K (previous section) assumed absolute thermal stability of the copper-hydrogen complexes at these temperatures. The close fit of the experimental DL depth profiles confirms this assumption. To check the Cu-H complex stability, the chemically etched (i.e., hydrogenated) samples were annealed at elevated temperatures and measured without additional etching. No DL centers were detected in a layer of several micrometers adjacent to the surface after the 200–400 °C anneals. Most probably, the electrically inactive Cu_s-H_3 complexes dominate in this layer. Increase of the annealing temperature to 500 °C results in the reappearance of the Cu_s levels, while the Cu-H complexes are not detected in these samples. Thus, the experimental results are in a good agreement with the theoretical predictions.

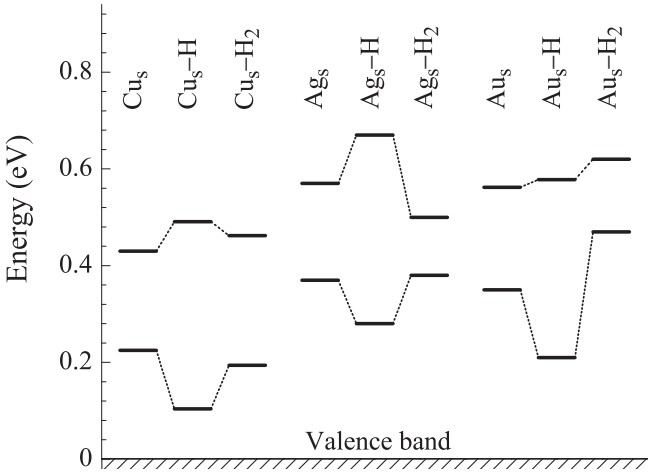

FIG. 6. Diagram of the donor and acceptor levels ascribed to the isoelectronic transition metals and their complexes with hydrogen. The data for copper, silver, and gold are from the present study, Ref. 9, and Refs. 6 and 7, respectively.

The electrical levels of the copper-hydrogen complexes were also calculated using the marker method.[4] The found DL pattern correctly reproduces the experimentally observed one: Both Cu_s-H_1 and Cu_s-H_2 complexes possess the donor and acceptor levels in the vicinity of those for the Cu_s center, while no deep levels are predicted for the Cu_s-H_3 complex. Moreover, the absolute level positions are also in a good agreement with the activation energies presented in Table I.

Figure 6 depicts the experimental data on the donor and acceptor levels of three isoelectronic transition metals (Cu, Ag, and Au) and their complexes with hydrogen. It is seen that the level patterns closely resemble each other. This striking similarity of the variations of the level positions due to the addition of hydrogen atoms (including the absence of electrical activity for the TM-H_3 complexes) provides additional support for the level identifications. Also, this suggests the same structure of the hydrogen-related complexes for these three metals.

V. SUMMARY

The standard DLTS and high-resolution Laplace-transform DLTS techniques are used for a thorough investigation of the process of substitutional copper hydrogenation in silicon. Hydrogen was introduced into the copper-doped crystals during wet chemical etching in an acid mixture and advanced deeper in the crystal by means of the reverse-bias annealing at 350–380 K. Four novel deep levels are observed to form

in the hydrogenated region at the expense of Cu_s levels (Table I). Because of the pairwise correlation of their concentration depth profiles, the levels are ascribed to two centers. The sum concentration of these two centers and remaining substitutional copper is nearly equal to the initial Cu_s concentration in the regions of weaker hydrogenation and decreases in the layers with the highest hydrogen concentration. We infer from these data that Cu_s forms complexes with one, two, and three hydrogen atoms; the first two are electrically active, while the last one introduces no levels in the lower half of the gap.

The above identification is strongly supported by the numerical modeling of successive Cu_s hydrogenation during the reverse-bias annealings. An accurate reproduction of the experimental depth profiles for all observed centers is achieved using a minimal number of fitting parameters: These are the radii of hydrogen capture to the corresponding centers in the neutral and negatively charged states (Table II). Further support is given by the comparison of the experimentally measured properties of the copper-hydrogen complexes with the results of theoretical calculations. Correctness of the identification of the observed levels is also confirmed by the striking similarity of the determined DL pattern with those reported for other (isoelectronic) metals and their complexes with hydrogen.

ACKNOWLEDGMENTS

This work was in part supported by the Deutsche Forschungsgemeinschaft under Grant No. LA 1397/7-1.

*nay@iptm.ru

[1]G. D. Watkins, Physica B **117-118**, 9 (1983).
[2]G. D. Watkins and P. M. Williams, Phys. Rev. B **52**, 16575 (1995).
[3]D. West, S. K. Estreicher, S. Knack, and J. Weber, Phys. Rev. B **68**, 035210 (2003).
[4]C. D. Latham, M. Alatalo, R. M. Nieminen, R. Jones, S. Öberg, and P. R. Briddon, Phys. Rev. B **72**, 235205 (2005).
[5]A. Carvalho, D. J. Backlund, and S. K. Estreicher, Phys. Rev. B **84**, 155322 (2011).
[6]E. O. Sveinbjörnsson and O. Engström, Appl. Phys. Lett. **61**, 2323 (1992); Phys. Rev. B **52**, 4884 (1995).
[7]A. L. Parakhonskii, O. V. Feklisova, S. S. Karelin, and N. Yarykin, Semiconductors **30**, 362 (1996).
[8]J.-U. Sachse, E. O. Sveinbjörnsson, W. Jost, J. Weber, and H. Lemke, Phys. Rev. B **55**, 16176 (1997); J.-U. Sachse, J. Weber, and E. O. Sveinbjörnsson, *ibid*. **60**, 1474 (1999).
[9]N. Yarykin, J.-U. Sachse, H. Lemke, and J. Weber, Phys. Rev. B **59**, 5551 (1999).
[10]J.-U. Sachse, J. Weber, and H. Lemke, Phys. Rev. B **61**, 1924 (2000).
[11]E. E. Haller, G. S. Hubbard, and W. L. Hansen, IEEE Trans. Nucl. Sci. **24**, 48 (1977).
[12]J.-U. Sachse, E. O. Sveinbjörnsson, N. Yarykin, and J. Weber, Mater. Sci. Eng. B **58**, 134 (1999).
[13]S. Knack, J. Weber, H. Lemke, and H. Riemann, Phys. Rev. B **65**, 165203 (2002).
[14]N. Yarykin and J. Weber, Semiconductors **47**, 275 (2013).
[15]T. Zundel and J. Weber, Phys. Rev. B **39**, 13549 (1989).
[16]H. B. Erzgräber and K. Schmalz, J. Appl. Phys. **78**, 4066 (1995).
[17]M. L. W. Thewalt, M. Steger, A. Yang, N. Stavrias, M. Cardona, H. Riemann, N. V. Abrosimov, M. F. Churbanov, A. V. Gusev, A. D. Bulanov, I. D. Kovalev, A. K. Kaliteevskii, O. N. Godisov, P. Becker, H.-J. Pohl, J. W. Ager III, and E. E. Haller, Physica B **401-402**, 587 (2007); M. Steger, A. Yang, N. Stavrias, M. L. W. Thewalt, H. Riemann, N. V. Abrosimov, M. F. Churbanov, A. V. Gusev, A. D. Bulanov, I. D. Kovalev, A. K. Kaliteevskii, O. N. Godisov, P. Becker, and H.-J. Pohl, Phys. Rev. Lett. **100**, 177402 (2008).
[18]L. C. Kimerling, J. Appl. Phys. **45**, 1839 (1974); D. Stievenard and D. Vuillaume, *ibid*. **60**, 973 (1986).
[19]L. Dobaczewski, P. Kaczor, I. D. Hawkins, and A. R. Peaker, J. Appl. Phys. **76**, 194 (1994); L. Dobaczewski, A. R. Peaker, and K. Bonde Nielsen, *ibid*. **96**, 4689 (2004).
[20]H. Lefévre and M. Schulz, Appl. Phys. **12**, 45 (1977).
[21]H. Lemke, Phys. Status Solidi A **95**, 665 (1986).
[22]S. D. Brotherton, J. R. Ayres, A. A. Gill, H. W. van Kesteren, and F. J. A. M. Greidanus, J. Appl. Phys. **62**, 1826 (1987).
[23]N. Yarykin and J. Weber, Phys. Rev. B **83**, 125207 (2011).
[24]Different amplitudes of the Cu_{100} and Cu_{220} peaks are seen also immediately after wet chemical etching without additional heat treatment [Fig. 1(a)]. That difference is determined by the Cu_{102} level of the Cu_s-Cu_i pair, which also introduces the Cu_{270} level.[13,14] Since Cu_{270} is low after RBA, the difference of the Cu_{100} and Cu_{220} amplitudes in Fig. 1(c) is due to another reason.
[25]O. V. Feklisova, E. B. Yakimov, N. Yarykin, and J. Weber, Semiconductors **35**, 1355 (2001).